

Article

Comparative genomics analysis of *bHLH* genes in cucurbits identifies a novel gene regulating cucurbitacin biosynthesis

Yuanchao Xu¹, Huimin Zhang², Yang Zhong^{1,3}, Naiyu Jiang², Xiaoyun Zhong¹, Qiqi Zhang¹, Sen Chai², Hongbo Li³ and Zhonghua Zhang^{2,*}¹Key Laboratory of Biology and Genetic Improvement of Horticultural Crops of the Ministry of Agriculture, Sino-Dutch Joint Laboratory of Horticultural Genomics, Institute of Vegetables and Flowers, Chinese Academy of Agricultural Sciences, Beijing 100081, China²Engineering Laboratory of Genetic Improvement of Horticultural Crops of Shandong Province, College of Horticulture, Qingdao Agricultural University, Qingdao 266109, China³Shenzhen Branch, Guangdong Laboratory for Lingnan Modern Agriculture, Shenzhen Key Laboratory of Agricultural Synthetic Biology, Genome Analysis Laboratory of the Ministry of Agriculture and Rural Affairs, Agricultural Genomics Institute at Shenzhen, Chinese Academy of Agricultural Sciences, Shenzhen 518120, China

*Corresponding author. E-mail: zhangzhonghua@qau.edu.cn

Abstract

The basic helix–loop–helix (bHLH) family of transcription factors (TFs) participate in a variety of biological regulatory processes in plants, and have undergone significant expansion during land plant evolution by gene duplications. In cucurbit crops, several *bHLH* genes have been found to be responsible for agronomic traits such as bitterness. However, the characterization of *bHLH* genes across the genomes of cucurbit species has not been reported, and how they have evolved and diverged remains largely unanswered. Here we identified 1,160 *bHLH* genes in seven cucurbit crops and performed a comprehensive comparative genomics analysis. We determined orthologous and paralogous *bHLH* genes across cucurbit crops by syntenic analysis between or within species. Orthology and phylogenetic analysis of the tandem-duplicated *bHLH* genes in the *Bt* cluster, which regulate the biosynthesis of cucurbitacins, suggest that this cluster is derived from three ancestral genes after the cucurbit-common tetraploidization event. Interestingly, we identified a new conserved cluster paralogous to the *Bt* cluster that includes two tandem *bHLH* genes, and the evolutionary history and expression profiles of these two genes in the new cluster suggest the involvement of one gene (*Brp*) in the regulation of cucurbitacin biosynthesis in roots. Further biochemical and transgenic assays in melon hairy roots supported the function of *Brp*. This study provides useful information for further investigating the functions of bHLH TFs and novel insights into the regulation of cucurbitacin biosynthesis in cucurbit crops and other plants.

Introduction

Basic helix–loop–helix (bHLH) transcription factors (TFs) are widespread in eukaryotes and constitute one of the largest TF families in plants [1]. Many studies suggest that the variety of cucurbit-common *bHLH* genes in plants were derived from one or a few predecessors through a significant number of gene duplications [2–4]. Segmental and tandem duplications or whole-genome duplications (WGDs) should contribute to the expansion of copy numbers in the bHLH family [5, 6]. In addition to the core-eudicot common hexaploidization (ECH) event, cucurbit crops also underwent an ancient cucurbit-common tetraploidization (CCT) event at ~90 million years ago (MYA) [7], and *Cucurbita* species have a recent WGD [8]. Which *bHLH* genes remained after these multiple duplication events and how they have evolved have not been investigated in cucurbit crops.

bHLH TFs can act as transcriptional activators or repressors and play essential roles in plant developmental and physiological processes, such as the regulation of flag leaf angle [9] and shoot branching [10], and responses to light [11], phytohormones [12], and low temperature [13]. Notably, many bHLH TFs regulate the biosynthesis of specialized secondary metabolites in plants [14–19], including cucurbitacins in cucumber (*Cucumis sativus*), melon (*Cucumis melo*), and watermelon (*Citrullus lanatus*) [17, 18]. Cucurbitacins are triterpenoids that confer a bitter taste in Cucurbitaceae plants [17]. The distinct cucurbitacins in cucurbits are structurally similar, and are synthesized mainly by conserved syntenic biosynthetic genes, which were reported to be regulated by a cluster (hereafter referred to as the *Bt* cluster) harboring several *bHLH*s [17, 18]. In cucumber, *Bt* (*Bitter fruit*) and *Bl* (*Bitter leaf*), located in the *Bt* cluster, can regulate

Received: 23 November 2021; Accepted: 30 January 2022; Published: 19 February 2022; Corrected and Typeset: 3 May 2022

© The Author(s) 2022. Published by Oxford University Press on behalf of Nanjing Agricultural University. This is an Open Access article distributed under the terms of the Creative Commons Attribution License (<https://creativecommons.org/licenses/by/4.0/>), which permits unrestricted reuse, distribution, and reproduction in any medium, provided the original work is properly cited.

the accumulation of cucurbitacin C (CuC) in fruits and leaves, respectively [17]. In melon and watermelon, the syntenic homologs of the Bt cluster were found to exert similar functions in diverse tissues by regulating cucurbitacin B (CuB) in melon and cucurbitacin E (CuE) in watermelon [18]. However, the evolutionary history and functional divergence of genes within the Bt cluster are largely unknown.

In this study, we identified and characterized 1,160 *bHLH* genes and performed a comparative evolutionary analysis in the seven cucurbit crops: cucumber, melon, watermelon, bottle gourd (*Lagenaria siceraria*), wax gourd (*Benincasa hispida*), bitter melon (*Momordica charantia*), and pumpkin (*Cucurbita pepo*). We determined orthologous and paralogous relationships among these *bHLH* genes and investigated features of *bHLH* tandem-duplicated genes (TDGs). Furthermore, we described the evolutionary history and divergence of the Bt cluster and reported the discovery of a novel functional *bHLH* gene regulating cucurbitacin biosynthesis in a Bt paralogous cluster. These results enhance our understanding of the biosynthetic regulation of secondary metabolites through TFs.

Results

Identification and classification of *bHLH* genes in seven cucurbit crops

By searching the genomes of seven cucurbits we identified 149 non-redundant *bHLH* genes in cucumber, 151 in melon, 154 in watermelon, 155 in bottle gourd, 150 in wax gourd, 150 in bitter melon, and 251 in pumpkin. All *bHLH* genes were numbered according to their genomic coordinates, yielding *CsabHLH001*–149, *CmebHLH001*–151, *ClabHLH001*–154, *LsibHLH001*–155, *BhibHLH001*–150, *MchbHLH001*–150, and *CmabHLH001*–251 (Supplementary Data Table S1). The number of *bHLH* genes was comparable among the cucurbit species investigated here, with the exception of pumpkin, whose genome encoded 1.67-fold more *bHLH* family members than the average number observed in the other six cucurbit crops, possibly due to a lineage-specific recent WGD event [8].

The basic region in the *bHLH* domain determines its DNA-binding activity [20]. Using previously published criteria [5], the *bHLH* TFs were divided into one group of DNA-binding proteins and another group of non-DNA-binding proteins (25.1–32.3% of all *bHLH* TFs). Furthermore, we subdivided the DNA-binding *bHLH* proteins into two subcategories as a function of their predicted cognate DNA-binding motif: E-box- and non-E-box-binding proteins (8.0–9.3% of all *bHLH* TFs). E-box-binding *bHLH* proteins were further subdivided into two groups: G-box-binding proteins (47.1–53.2% of all *bHLH* TFs) and non-G-box-binding proteins (11.0–13.3% of all *bHLH* TFs) (Fig. 1a).

Intron and exon structures can help elucidate the phylogenetic relationships of a gene family. We identified 12 different intron distribution patterns based on the

number (zero to three) and relative positions of introns within the region encoding the *bHLH* domain (designated I–XI and O; Fig. 1b). About 80% of the identified *bHLH*s featured the three most common patterns: I, IX, and XI. Pattern IX was the most common, with only one intron in the loop region. Pattern I was characterized by three introns at three highly conserved positions and was the second most common pattern. Finally, pattern XI, with no intron in the *bHLH* domain-encoding region, was the third most common pattern (Fig. 1b). The intron distribution patterns in cucurbit crops are like those in tomato (*Solanum lycopersicum*) [21] and Arabidopsis (*Arabidopsis thaliana*) [5], suggesting that this might be a common feature among plant species.

Evolution of *bHLH* genes in seven cucurbit crops

To understand the phylogenetic relationships among *bHLH*s in cucurbit crops, we constructed an unrooted neighbor-joining phylogenetic tree using a multiple alignment of the *bHLH* domain. The 1,160 cucurbit *bHLH* genes are clustered into 28 subfamilies according to the classification of Arabidopsis *bHLH*s [22] (Fig. 2a; Supplementary Data Fig. S1). In most subfamilies, DNA-binding properties, intron pattern distributions, and motif architectures of *bHLH* genes were relatively conserved (Supplementary Data Fig. S1), suggesting the reliability of the classification and phylogenetic tree of cucurbit *bHLH* genes presented here.

To further investigate the evolutionary trajectory of the *bHLH* family, we constructed a syntenic map and generated a syntenic gene list of *bHLH* genes across the seven cucurbit crops (Fig. 2b; Supplementary Data Table S2). Most highly conserved syntenic blocks were shared by the seven cucurbit genomes, with ~90% of all *bHLH* genes mapping to these orthologous blocks. For instance, >10 orthologous *bHLH* genes formed a superblock that was perfectly matched in all seven cucurbit crop genomes, as represented by the magenta lines in Fig. 2b. We next clustered and identified 151 *bHLH* orthologous groups (OGs) present in at least two cucurbit genomes (Supplementary Data Table S2, OG001–151) and 13 species-specific *bHLH* OGs (Supplementary Data Table S2, OG152–164). In 92% of all OGs, *bHLH* TFs from each cucurbit crop exhibited the same DNA-binding ability and their encoding genes showed the same intron distribution pattern (Supplementary Data Table S2).

We then identified paralogous gene pairs: 28 pairs in cucumber, 28 pairs in melon, 31 pairs in watermelon, 25 pairs in bottle gourd, 14 pairs in wax gourd, 33 pairs in bitter melon, and 129 pairs in pumpkin (Supplementary Data Fig. S2 and Supplementary Data Table S3). About 94% of these paralogous *bHLH* TFs shared the same DNA-binding ability and their encoding genes showed the same intron distribution pattern (Supplementary Data Fig. S2). All paralogous *bHLH* gene pairs had non-synonymous substitutions/synonymous substitutions (K_a/K_s) values <0.6 (Supplementary Data Fig. S3), suggesting that the majority of paralogous

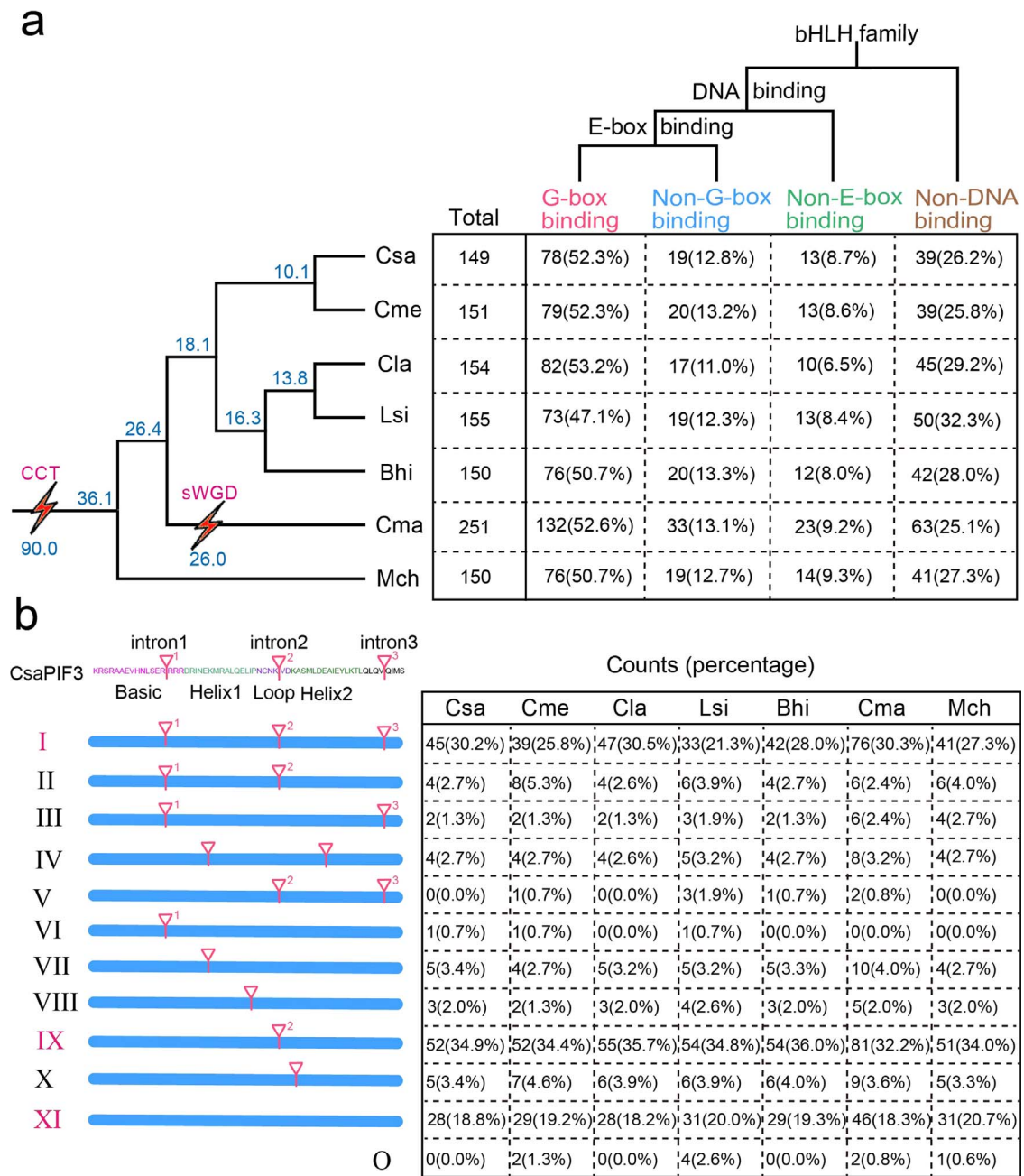


Figure 1. DNA-binding ability and conserved intron distribution patterns of *bHLH* genes in seven cucurbit crops. **a** Predicted DNA-binding characteristics based on the amino acid sequences of the *bHLH* domain. A species tree of seven cucurbits is shown on the left. Csa, cucumber; Cme, melon; Cla, watermelon; Lsi, bottle gourd; Bhi, wax gourd; Cma, pumpkin; Mch, bitter gourd; sWGD: specific whole-genome duplication. Blue numbers show the estimated divergence time of each node or occurrence time of WGD. **b** Intron distribution patterns within the *bHLH* domain of seven cucurbit crops. The positions of introns are indicated by triangles and numbered 1–3 based on the *bHLH* region of *CsaPIF3* (*CsaV3_2G007370*), which is shown at the top. The count and percentage of *bHLH*s displaying each pattern in seven cucurbit crops are given in the table on the right.

bHLH genes have undergone purifying selection. These paralogous genes might be the extant product of WGDs during the evolutionary history of cucurbit crops. These results offer novel insights into the evolution of *bHLH* genes in cucurbit crops.

Characterization of *bHLH* tandem-duplicated genes

Local gene duplication generates TDGs and is ubiquitous during genome evolution [23]. To explore the features and

potential functions of *bHLH* TDGs, we identified clusters of *bHLH* TDGs—10 genes in cucumber (four clusters); 9 in melon (three clusters); 14 in watermelon (five clusters); 15 in bottle gourd (seven clusters); 10 in wax gourd (four clusters); 10 in bitter gourd (four clusters); and 8 in pumpkin (four clusters)—based on chromosome localization of the genes and sequence similarity of the encoded proteins (Supplementary Data Fig. S4; Table 1). TDG clusters were named according to their order in their genomic coordinates, such as ‘T1’ and ‘T2’

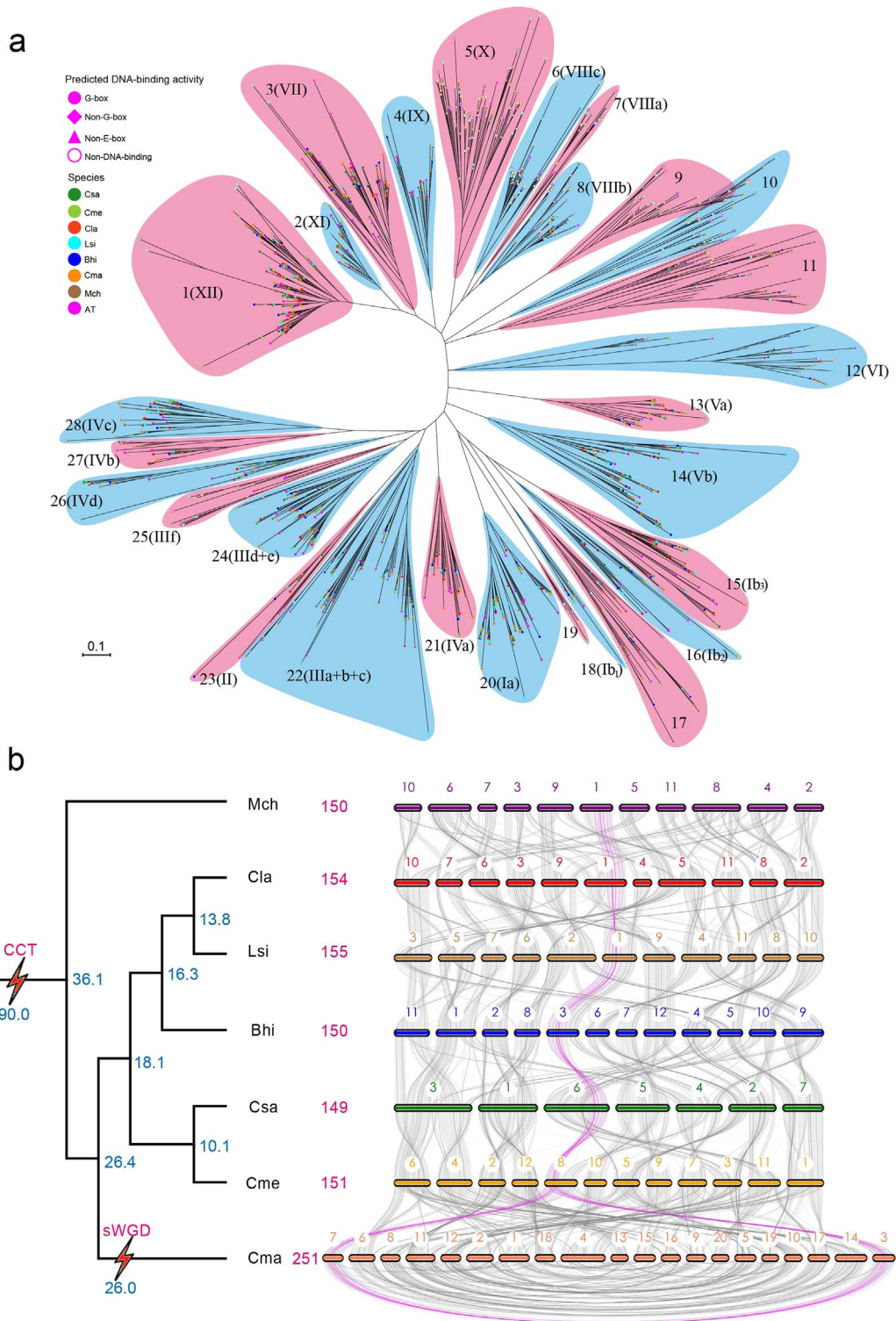


Figure 2. Evolution of *bHLH* genes in seven cucurbit crops. **a** Unrooted neighbor-joining phylogenetic tree of 1,322 *bHLH*s from cucumber, melon, watermelon, bottle gourd, wax gourd, pumpkin, bitter gourd, and arabidopsis. *bHLH*s are divided into 28 subfamilies. The Roman numerals in brackets denote subfamilies, as defined in arabidopsis. Detailed information on the phylogenetic tree is given in [Supplementary Data Fig. S1](#). **b** Syntenic analysis of *bHLH* genes among seven cucurbit crops. A species tree of seven cucurbits is shown on the left. sWGD, specific whole-genome duplication. Blue numbers are estimated divergence times (in millions of years ago) of each node or occurrence time of WGD. Magenta numerals are the numbers of *bHLH* genes in each cucurbit crop. Magenta and gray lines display the collinear *bHLH* genes among seven cucurbit crop genomes. The light gray lines denote collinear blocks.

([Supplementary Data Fig. S4](#)). The numbers of *bHLH* TDGs varied across the seven cucurbit crops, with more *bHLH* TDGs in watermelon and bottle gourd than in

the other five species. The K_s values for each TDG pair belonging to the same cluster were then calculated to trace their divergence time after duplication

Table 1. List of orthologous gene groups of TDGs among seven cucurbit crops

Orthologous group	Melon	Cucumber	Watermelon	Wax gourd	Bottle gourd	Bitter gourd	Pumpkin
OG001	<i>CmebHLH104*</i> <i>CmebHLH105*</i> <i>CmebHLH106*</i>	<i>CsabHLH125*</i> <i>CsabHLH126*</i> <i>CsabHLH127*</i>	<i>ClabHLH009*</i> <i>ClabHLH010*</i> <i>ClabHLH011*</i>	<i>BhibHLH041*</i> <i>BhibHLH042*</i> <i>BhibHLH043*</i>	<i>LsibHLH007*</i> <i>LsibHLH008*</i> <i>LsibHLH009*</i>	<i>MchbHLH004*</i> <i>MchbHLH005*</i>	<i>CmabHLH030*</i> <i>CmabHLH031*</i> <i>CmabHLH086*</i> <i>CmabHLH087*</i>
OG002	<i>CmebHLH112</i>	<i>CsabHLH087*</i> <i>CsabHLH088*</i>	<i>ClabHLH049*</i> <i>ClabHLH050*</i> <i>ClabHLH051*</i>	<i>BhibHLH048*</i> <i>BhibHLH049*</i> <i>BhibHLH050*</i>	<i>LsibHLH013*</i> <i>LsibHLH014*</i>	<i>MchbHLH001</i>	<i>CmabHLH024</i> <i>CmabHLH091</i>
OG003	<i>CmebHLH120*</i> <i>CmebHLH121*</i> <i>CmebHLH122*</i> <i>CmebHLH123*</i>	<i>CsabHLH093*</i> <i>CsabHLH094*</i> <i>CsabHLH095*</i>	<i>ClabHLH001*</i> <i>ClabHLH002*</i> <i>ClabHLH003*</i> <i>ClabHLH004*</i>	<i>BhibHLH135*</i> <i>BhibHLH136*</i>	<i>LsibHLH120*</i> <i>LsibHLH121*</i> <i>LsibHLH122*</i> <i>LsibHLH123*</i>	<i>MchbHLH077*</i> <i>MchbHLH078*</i>	<i>CmabHLH017</i> <i>CmabHLH194*</i> <i>CmabHLH195*</i>
OG004	<i>CmebHLH082*</i> <i>CmebHLH083*</i>	<i>CsabHLH064*</i> <i>CsabHLH065*</i>	<i>ClabHLH064*</i> <i>ClabHLH065*</i>	<i>BhibHLH008*</i> <i>BhibHLH009*</i>	<i>LsibHLH071*</i> <i>LsibHLH072*</i>	<i>MchbHLH128</i>	<i>CmabHLH231</i> <i>CmabHLH197</i>
OG005	<i>CmebHLH138</i>	<i>CsabHLH111</i>	<i>ClabHLH079*</i> <i>ClabHLH080*</i>	<i>BhibHLH145</i>	<i>LsibHLH132</i>	<i>MchbHLH146</i>	<i>CmabHLH210</i>
OG006	<i>CmebHLH037</i>	<i>CsabHLH117</i>	<i>ClabHLH113</i>	<i>BhibHLH058</i>	<i>LsibHLH109*</i> <i>LsibHLH110*</i>	<i>MchbHLH088</i>	<i>CmabHLH054</i> <i>CmabHLH148</i>
OG007	<i>CmebHLH079</i>	<i>CsabHLH061</i>	<i>ClabHLH061</i>	<i>BhibHLH005</i>	<i>LsibHLH076*</i> <i>LsibHLH077*</i>	<i>MchbHLH052</i>	<i>CmabHLH182</i>
OG008	<i>CmebHLH039</i>	<i>CsabHLH049</i>	<i>ClabHLH115</i>	<i>BhibHLH057</i>	<i>LsibHLH113</i>	<i>MchbHLH091*</i> <i>MchbHLH092*</i>	<i>CmabHLH057</i>
OG009	<i>CmebHLH066</i>	<i>CsabHLH036</i>	<i>ClabHLH150</i>	<i>BhibHLH083</i>	<i>LsibHLH148</i>	<i>MchbHLH105*</i> <i>MchbHLH106*</i> <i>MchbHLH107*</i> <i>MchbHLH108*</i>	No gene
OG010	<i>CmebHLH141</i>	<i>CsabHLH016</i>	<i>ClabHLH039</i>	<i>BhibHLH148</i>	<i>LsibHLH025</i>	No gene	<i>CmabHLH224*</i> <i>CmabHLH225*</i>
Number of TDGs (clusters)	9 (three)	10 (four)	14 (five)	10 (four)	15 (seven)	10 (four)	8 (four)

*TDGs.

(Supplementary Data Table S4). In watermelon and bottle gourd, we obtained two (T1 and T5) and three (T4, T5, and T6) gene pairs with K_s values <0.32 , suggesting that these TDGs may emerge recently after the divergence between the two species (Supplementary Data Table S4). This might explain the higher number of *bHLH* TDGs in these two species. Pumpkin, which underwent a recent WGD event, had the smallest number of *bHLH* TDGs, despite having the largest *bHLH* gene family among the seven cucurbits (Table 1; Supplementary Data Fig. S4 and Supplementary Data Table S4). Considering WGD events may accelerate the loss of TDGs [24], we speculate that the evolution of TDGs in pumpkin might have been affected by the recent WGD event [8].

Furthermore, we investigated the distribution of TDGs in OGs and their potential functions. All TDGs were distributed in 10 OGs (Table 1), including four (OG001, OG002, OG003, and OG004) in which we detected TDG clusters in at least four cucurbit crops. Homologous genes in arabidopsis for these TDG cluster genes in OG001 and OG002 were reported to be involved in the regulation of iron homeostasis [25, 26]. OG003 included the Bt cluster, which regulates cucurbitacin biosynthesis in different tissues in cucumber, melon, and watermelon [17, 18], whereas the function of genes in OG004 remains to be elucidated in cucurbits.

Evolution and divergence of the Bt cluster

In cucumber, melon, and watermelon, the Bt cluster regulates cucurbitacin biosynthesis in different tissues [17, 18]. To explore the evolution and divergence of this cluster across more cucurbit crops, we performed a comprehensive comparative genomic analysis by assessing local synteny of paralogous or orthologous genes, as well as constructing a phylogenetic tree and analyzing gene expression patterns. Syntenic paralogous gene analysis detected a paralogous cluster (OG004 in Table 1) of the Bt cluster in cucurbit crops (Fig. 3a; Supplementary Data Fig. S5 and Supplementary Data Table S5). The K_s values of each paralogous gene pair mapping to the Bt cluster were much smaller than those of all gene pairs between clusters (Fig. 3b; Supplementary Data Fig. S6). The phylogenetic tree showed that the evolutionary distance between genes in the Bt cluster is closer than that of genes between clusters (Fig. 3b). These results suggested that the Bt cluster in cucurbits might have arisen after the CCT event [7] (Fig. 3b; Supplementary Data Fig. S6). By local syntenic orthologous gene analysis, we found that the Bt cluster is collinearly distributed among the Cucurbitaceae crops, as is its paralogous cluster (Fig. 3c and d). In the paralogous cluster, the number of genes appears to be conserved, with two genes in each

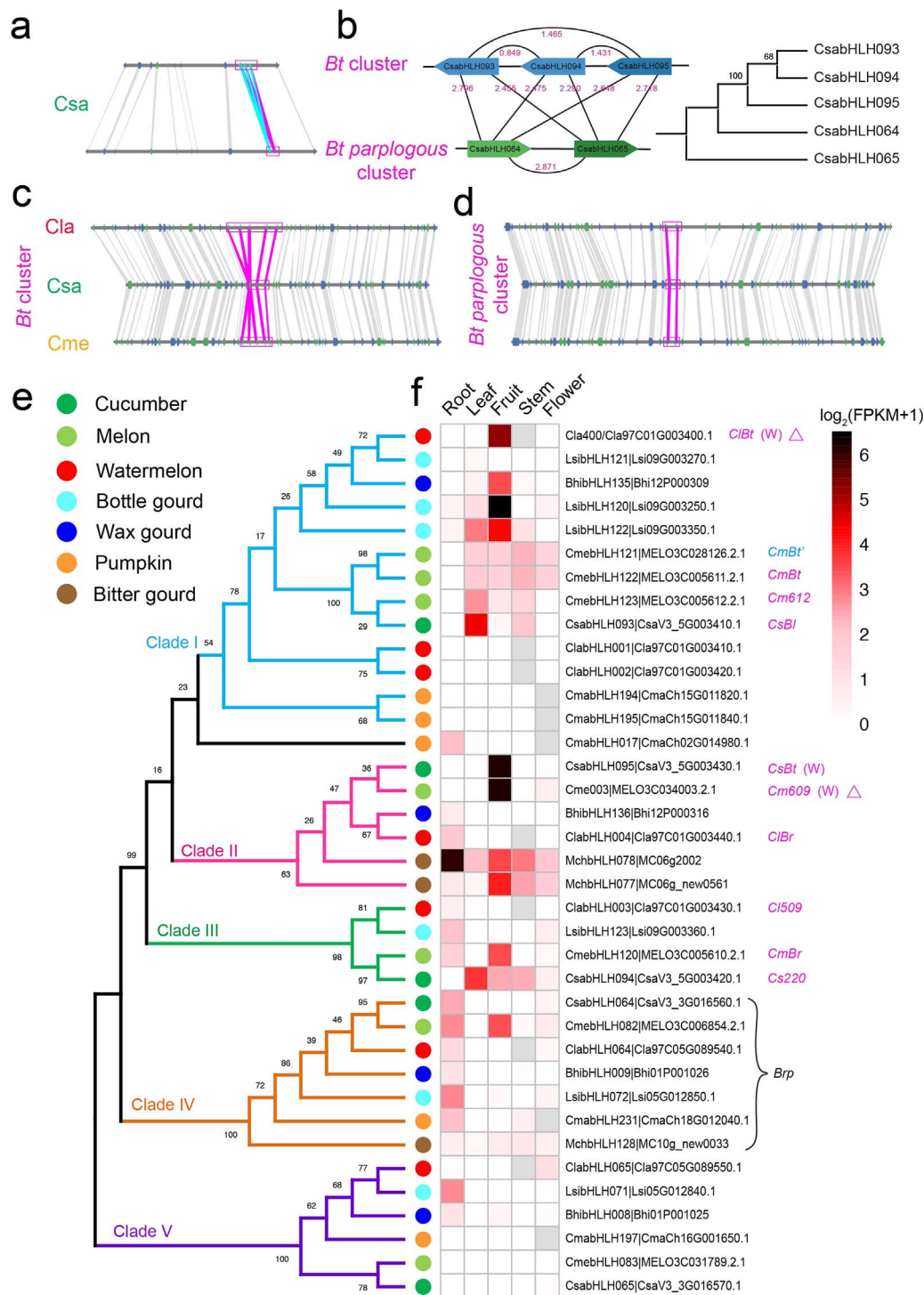


Figure 3. Evolution and divergence of the Bt cluster. **a** The syntenic block between the Bt cluster and its paralogous cluster in cucumber. **b** Evolution of the Bt cluster and its paralogous cluster in cucumber. The magenta numbers are K_s values. **c, d** Syntenic regions of the Bt cluster (**c**) and its paralogous cluster (**d**) among cucumber (*Csa*), melon (*Cme*), and watermelon (*Cla*). **e, f** Phylogenetic tree (**e**) and expression heat maps (**f**) of genes in the Bt cluster and its paralogs. Gray boxes indicate missing values. The magenta 'W' means genes only expressed in fruits of wild accessions. The magenta abbreviations are the same as in reference 18. Triangles mean premature translational termination. The CDSs of *CmBt* and *CmBt'* are identical. One gene in the Bt paralogous cluster, exhibiting high expression in the roots of cucurbit crops, is designated *Brp*.

species (Fig. 3d). However, the gene numbers in the Bt cluster were much more flexible, with three genes in cucumber, five genes in melon, five genes in watermelon, four genes in bottle gourd, and two genes in wax gourd in the Bt cluster (Fig. 3c; Supplementary Data Fig. S6). To infer the number of ancestral genes in the Bt cluster and

their evolution, we divided *bHLH* genes from the Bt cluster and its paralogous cluster from the seven cucurbit species into five major clades (Clades I–V) based on the phylogenetic tree (Fig. 3e). The genes from the Bt cluster were distributed in Clades I, II, and III (Fig. 3e), suggesting three ancestral genes in the Bt cluster after the CCT

event. In cucumber, three *Bt* cluster genes remained in Clades I, II, and III. However, new members appeared in Clade I for watermelon, melon, and bottle gourd after species diversification, based on the intraspecies and interspecies K_s values and phylogenetic analysis (Fig. 3e; Supplementary Data Figs S6 and S7). For example, the K_s values of each pair among *CmebHLH121*, *CmebHLH122*, and *CmebHLH123* in the *CmeBt* cluster were smaller than interspecies K_s values, suggesting that these three genes arose in melon after its divergence from the other species (Supplementary Data Figs S6 and S7). In addition, several members of Clade II or Clade III were lost in some cucurbit crops: wax gourd lacked a gene in Clade III (Fig. 3e). Finally, we inferred the evolutionary correspondence of *Bt* cluster genes among the seven cucurbit species (Supplementary Data Table S6).

The expression patterns of genes in the *Bt* cluster and its paralogous cluster showed a high degree of tissue specificity. For example, *ClA400*, *BhibHLH135*, *LsibHLH120*, *CsabHLH095* (*CsBt*), *Cme003*, and *MchbHLH077* were predominantly expressed in fruits, while *CsabHLH093* (*CsBl*) exhibited a leaf-specific expression pattern and *CmabHLH017*, *ClabHLH004*, *LsibHLH123*, *CsabHLH064*, and *LsibHLH071* were mainly expressed in roots (Fig. 3f). These expression patterns imply the potential functions of the respective *bHLH* genes in specific tissues, echoing the expression of *CsBt* and *CsBl* in cucumber fruits and leaves and their role in regulating cucurbitacin biosynthesis, respectively [17, 18]. Notably, most genes in Clade IV were highly expressed in roots (Fig. 3f), suggesting their potential roles in regulating cucurbitacin biosynthesis in this tissue.

A novel functional *bHLH* gene of the *Bt* paralogous cluster regulates cucurbitacin biosynthesis in roots

We found that one gene in the *Bt* paralogous cluster of each cucurbit crop, belonging to Clade IV, exhibited a high level of expression in roots (designated *Brp*; Fig. 3e and f). Given its evolutionary history, we hypothesized that *Brp* might be involved in regulating the biosynthesis of cucurbitacins in the roots of cucurbit crops. To explore the function of *Brp* in cucurbits, we conducted heterologous transient expression experiments in *Nicotiana benthamiana* leaves, using a reporter construct consisting of the promoter from the Bitter (*Bi*) locus of melon and watermelon, driving the expression of the firefly luciferase (*LUC*) gene. Here the *Bi* gene encodes oxidosqualene cyclase, which catalyzes the first step of cucurbitacin biosynthesis (Supplementary Data Fig. S8) [18]. Compared with the control, the normalized transcriptional activity [ratio of firefly luciferase to *Renilla* luciferase (*LUC/REN*)] of pro*Bi*:*LUC* was significantly promoted by transient overexpression of *Brp* from melon (*CmebHLH082*) and watermelon (*ClabHLH064*) (Fig. 4a–c).

To better understand the underlying function of *Brp* in cucurbit crops, we generated *CmeBrp*-overexpressing

(*CmeBrp*-OE) transgenic hairy melon roots with *CmeBrp* expression driven by the constitutive cauliflower mosaic virus (CaMV) 35S promoter (Fig. 4d). We also produced transgenic hairy melon roots of CRISPR/Cas9 (*cr*)-mediated *CmeBrp* knockout mutants (*CmeBrp-cr*) (Fig. 4d and e). We then quantified cucurbitacin B (CuB) contents in hairy roots of the wild-type (WT), *CmeBrp-cr*, and *CmeBrp*-OE lines, which revealed a drastic increase in CuB contents in *CmeBrp*-OE lines and a significant decrease in *CmeBrp-cr* lines compared with the WT (Fig. 4f; Supplementary Data Fig. S9). Real-time quantitative polymerase chain reaction (RT-qPCR) analysis indicated that the expression of *CmeBrp* and four key biosynthetic genes of CuB (*CmeBi*, *Cme890*, *Cme180*, and *CmeACT*; Supplementary Data Fig. S8) [18] were markedly upregulated in the *CmeBrp*-OE lines compared with the WT (Fig. 4g–k), whereas the expression of four key biosynthetic genes of CuB were substantially lower in the *CmeBrp-cr* lines relative to the WT (Fig. 4h–k). In summary, these results suggest that *CmeBrp* may regulate the biosynthesis of cucurbitacin B in melon roots.

Discussion

Comparative genomics analysis can be powerful approaches to provide novel insights into gene function and evolution. In this study, we performed comparative genomics analysis of *bHLH* genes in seven cucurbit species and inferred the evolution and divergence of the *Bt* cluster. Together with evolutionary relationships and expression profiles, these results empowered the discovery of a novel gene regulating cucurbitacin biosynthesis. The methodology applied in this research presents an example of how gene family analysis facilitates functional gene studies.

Tandem duplications are a widespread phenomenon in plant genomes and play significant roles in evolution and adaptation to changing environments [27]. Compared with WGD-derived duplicate genes, TDGs provide a continuous supply of variants available for adaptation to continuously changing environments [28]. Even though the number of *bHLH* genes is the highest in pumpkin compared with that in other cucurbit crops, it has the fewest *bHLH* TDGs. Both TDGs and WGDs can lead to the expansion of gene families and increase gene diversity. During pumpkin evolution, WGD may have provided additional genetic material and increased gene diversity, and thus the fraction of lost tandem arrays was significantly larger than that of lost non-tandem genes [24]. Therefore, we hypothesize that TDGs in pumpkin were dramatically lost after the recent WGD, which might have resulted from a gene dosage effect.

Compared with the metabolic biosynthetic gene clusters [29–32], the TF clusters governing these metabolic enzymes are less identified and characterized [33]. Unlike the metabolic biosynthetic clusters, which include genes encoding various classes of metabolic enzymes [34, 35],

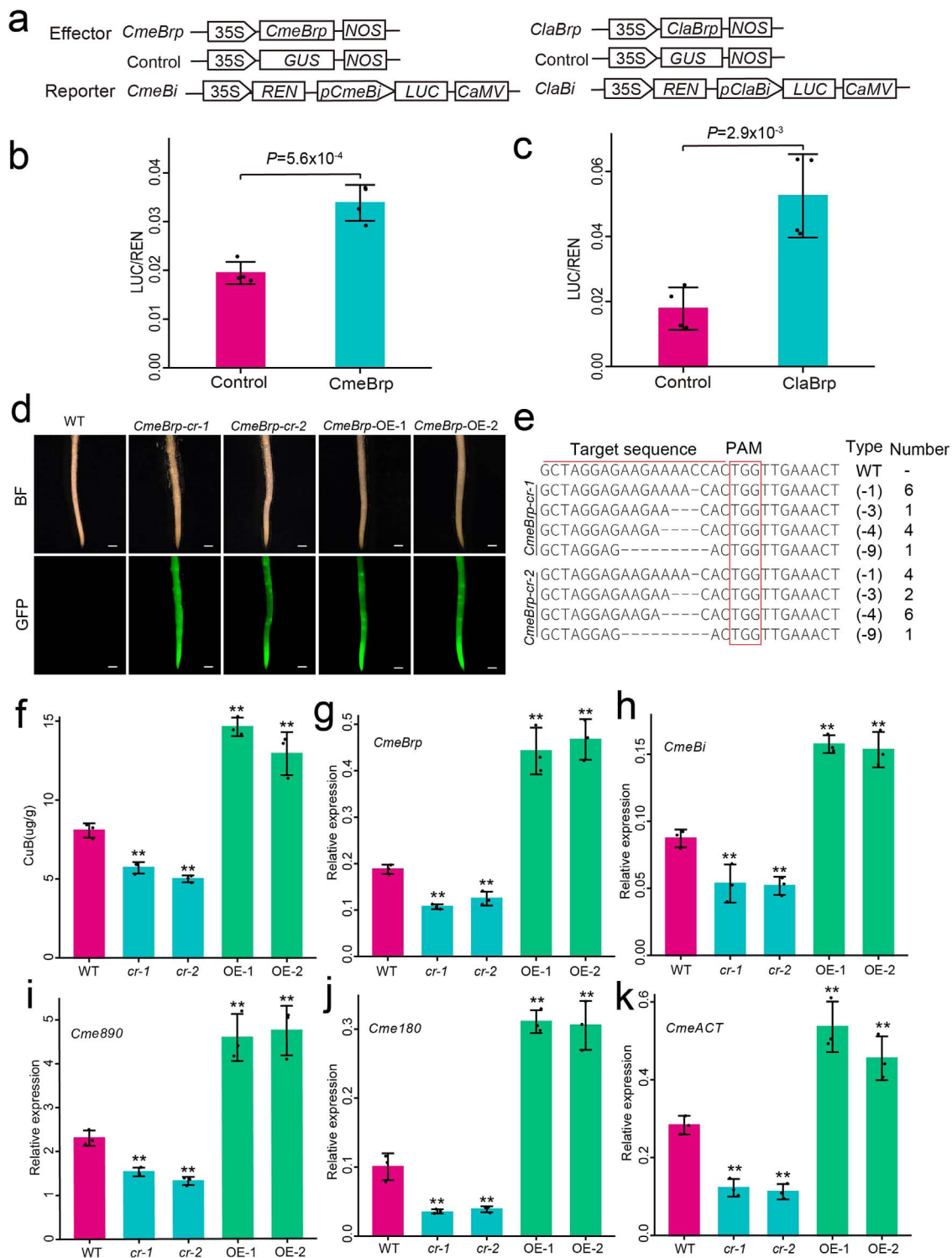


Figure 4. *Brp* participates in regulating cucurbitacin biosynthesis. **a** Schematic diagram showing the constructs used in the transient transcriptional activity assays. **b, c** *Brp* activates *Bi* expression in a tobacco leaf assay system for melon (**b**) and watermelon (**c**). Values are mean \pm standard deviation from four biological replicates. **d** GFP signals detected in hairy roots of *CmeBrp*-overexpressing and *CmeBrp* knockout lines. Scale bar = 1 mm. **e** Sequence analysis of *CmeBrp* in two knockout lines. A total of 25 colonies were sequenced in *CmeBrp*-*cr* lines. Mutant types and numbers are showed at right. **f** Content of CuB in WT, *CmeBrp* knockout, and *CmeBrp* overexpressing lines. **g** Relative expression of *CmeBrp* in WT, *CmeBrp* knockout, and *CmeBrp*-overexpressing lines. **h–k** Relative expression of four key CuB biosynthetic genes, *CmeBi* (**h**), *Cme890* (**i**), *Cme180* (**j**), and *CmeACT* (**k**), in WT, *CmeBrp* knockout, and *CmeBrp*-overexpressing lines. Transcript levels were measured by RT-qPCR. Values are represented as mean \pm standard deviation from three biological replicates. ****** $P < .01$, Student's *t*-test.

TFs in the same cluster may have overlapping or distinct regulatory functions. In Madagascar periwinkle (*Catharanthus roseus*), three clustered *bHLH* genes [named *BIS1*

(*bHLH indoid synthesis 1*), *BIS2*, and *BIS3*] regulate iridoid biosynthesis in the terpenoid indole alkaloid biosynthetic pathway [36–38]. However, the origin, copy number, and

evolution of TF clusters are largely unknown [38]. In this study, we determined that gene number within the Bt cluster is variable across species, and a novel bHLH cluster consisting of two genes that is relatively conserved and paralogous to the Bt cluster also regulates cucurbitacin biosynthesis. These *bHLH* genes belonged to the 15(Ib3) subfamily (Supplementary Data Fig. S1). Although the functions of *AtbHLHs* belonging to the 15(Ib3) subfamily were unknown in arabidopsis, these *AtbHLHs* clustered with *Brps* into a clade and were highly expressed in roots. Therefore, we speculated that the Bt paralogous cluster is an ancestral cluster, as evidenced by the higher K_s values of each pair of genes in the Bt paralogous cluster (Fig. 3b; Supplementary Data Fig. S6). These findings will help in understanding the function and evolution of TF clusters.

Materials and methods

Data collection and identification of *bHLH* genes in seven cucurbit crops

Melon genome sequence data were obtained from the Melonomics database (www.melonomics.net), bitter melon genome sequence data were obtained from <https://db.cngb.org/search/assembly/CNA0000004/>, and for the other five cucurbit crops (cucumber, watermelon, wax gourd, bottle gourd, and pumpkin) genome sequence data were obtained from <http://cucurbitgenomics.org>. Information and sequences for *A. thaliana* *bHLHs* (*AtbHLHs*) were retrieved from <https://www.arabidopsis.org>. The *bHLH* proteins of seven cucurbit crops (*CsabHLHs*, *CmebHLHs*, *ClabHLHs*, *BhibHLHs*, *LsibHLHs*, *CmabHLHs*, and *MchbHLHs*) were predicted using the HLH hidden Markov model (HMM) profile obtained from Pfam (<http://pfam.xfam.org>, PF00010) and used as queries to search the *bHLH* proteins from cucurbit crop sequences with HMMER (version 3.1b2) software (<http://hmmer.janelia.org>). We also performed a BLASTP search against the *AtbHLH* database. Redundant protein sequences were removed by searching in the NCBI database (<https://www.ncbi.nlm.nih.gov/Structure/bwrpsb/bwrpsb.cgi>) and the SMART database (<http://smart.embl-heidelberg.de>). In addition, some *bHLH* genes were re-annotated, due to errors existing in the raw annotation, by *ab initio* prediction, transcript mapping, and evidence from other reference genome versions.

Multiple alignments and phylogenetic analysis

Multiple sequence alignments of identified *bHLH* domains of 162 arabidopsis (*AtbHLH*), 149 cucumber (*CsabHLH*), 151 melon (*CmebHLH*), 154 watermelon (*ClabHLH*), 150 wax gourd (*BhibHLH*), 155 bottle gourd (*LsibHLH*), 251 pumpkin (*CmabHLH*), and 150 bitter melon (*MchbHLH*) *bHLH* proteins were carried out using MUSCLE software with default parameters. To visualize the conserved motifs, the sequences were analyzed with WEBLOGO programs (<http://weblogo.berkeley.edu>) based on the result of each cucurbit crop multiple sequence

alignment. Based on the results of all seven cucurbit crops and arabidopsis multiple sequence alignments, a neighbor-joining tree was constructed using MEGA 7.0 [39] using a bootstrap test with 1,000 replicates based on the Jones–Taylor–Thornton (JTT) model and 80% partial deletion for gap treatment. The phylogenetic tree was visualized in MEGA 7.0.

DNA-binding ability analysis

Firstly, based on multiple sequence alignments of *bHLH* domains proteins, we identified conserved amino acid residues in the *bHLH* domains and four conserved motifs including one basic motif, two amphipathic α -helices, and one loop that linked the two amphipathic α -helices (Supplementary Data Fig. S10 and Supplementary Data Table S7). Then we defined proteins with more than five basic amino acid residues in the basic region as DNA-binding proteins based on the criteria developed by Toledo-Ortiz *et al.* [5]. The *bHLH* proteins were divided into a group of DNA-binding proteins and a group of non-DNA-binding proteins. Furthermore, the DNA-binding proteins were subdivided into two subcategories, E-box (based on the presence of E-2 and R-4) and non-E-box-binding proteins (without the simultaneous presence of E-2 and R-4). Then E-box-binding proteins were further subdivided into two groups, including G-box-binding proteins (H/K-1, E-2, and R-5 were required) and non-G-box-binding proteins. Consensus amino acids and the numbers of them, such as E-2, are described in Supplementary Data Table S7.

Gene structure analysis and protein motif detection

The exon/intron organization and splicing phase of the predicted *bHLHs* were investigated based on the GFF/GTF annotation files of seven cucurbit crop genomes. Furthermore, to discover the intron distribution pattern, we did alignment analysis with the coding sequence of the *bHLH* domain and genome sequences using Blat software [40]. Then exon/intron structures, the splicing phase, and different regions of the *bHLH* domain were graphically displayed using the Gene Structure Display Server [41] (GSDS, <http://gsds.cbi.pku.edu.cn/>). To analyze other conserved motifs in the complete amino acid sequences of *bHLHs*, the protein sequences of candidate *bHLHs* were analyzed using MEME [42] (version 5.1.1) software (<http://meme-suite.org/tools/meme>). The parameter settings were: number of motifs to find, 15; minimum width of motifs, 6; maximum width of motifs, 50.

Identification of orthologous genes among seven cucurbit crops and paralogous genes in each cucurbit crop

Gene synteny analysis by MCScanX [43]) with default parameters. Based on the syntenic blocks, each inter-genomic *bHLH* orthologous genes among seven cucurbit crops were identified. Then we merged the orthologous

gene pair information using a python script. Visualizations of orthologous genes were generated using jcv (https://github.com/tanghaibao/jcv). Similarly, intra-genomic *bHLH* paralogous genes were identified. Paralogous genes were graphically displayed as circos figures.

Chromosomal locations and tandem-duplicated gene detection

The chromosomal positions of *bHLH* loci were obtained from each cucurbit crop general feature format (GFF) or gene transfer format (GTF) gene structure annotation files. The distribution of *bHLH* genes on chromosomes in each cucurbit crop was drawn using TBtools software [44]. Tandem genes were detected using SynOrths [45] and MCscanX [43] softwares the with default parameters.

K_a , K_s and K_a/K_s analysis

The non-synonymous substitutions (K_a), synonymous substitutions (K_s), and K_a/K_s values of paralogous gene pairs and tandem array genes (between any two genes in the same tandem-duplicated gene cluster) were calculated using KaKs_Calculator [46].

Gene expression analyses of *bHLH* genes in seven cucurbit crops

RNA-seq data for the *bHLH* genes were obtained from previous studies of differential gene expression in organs and tissues in seven cucurbit crops [8, 47–52]. All clean RNA-seq reads from each sample were mapped onto the corresponding genome sequences, using Hisat2 [53] (version 2.1.0) with default parameters. The generated BAM format alignments, together with the gene GTF annotation file, were then fed to StringTie (v1.3.4d) software to compute FPKM (the fragments per kilobase of exon model per million reads mapped) values of genes [54] (v1.3.4d). Finally, the \log_2 -transformed (FPKM + 1) values were used to generate a heat map by R.

Dual-luciferase assay

The full-length coding sequence (CDS) of *Brp* was inserted into the pBI121 plasmid to generate the *Brp*-pBI121 effector, while the 2000-bp sequence upstream of the translation initiation start site of the *Bi* gene was cloned into the pGreen II 0800-LUC to generate pBi-LUC double-reporter vector. The *Brp*-pBI121 effector and pBi-LUC reporter vector were transformed into *Agrobacterium tumefaciens* strain GV3101 and GV3101(pSoup-p19), respectively. The reporter and effector were co-infiltrated into *N. benthamiana* leaves at a volume ratio of 9:1. The empty pBI121 vector was used as control. The leaf samples were collected within 60 hours after injection to measure luciferase activities using the Dual-Luciferase Reporter Assay System (Promega, USA, E1910) using a GloMax 20/20 Luminometer (Promega, USA) according to the manufacturer's instructions (Promega, USA). The relative reporter gene expression levels were expressed as the LUC/REN ratio. Four independent transformations for each sample were performed.

Agrobacterium rhizogenes-mediated hairy root transgenic system in melon

To construct the *CmeBrp* overexpression vector, the full-length CDS of *CmeBrp* was cloned into the pCAM-BIA1305.4 binary vector, using an In-Fusion HD Cloning Kit (Clontech). To generate the CRISPR/Cas9 editing vector, the 19-bp sgRNA fragment of *CmeBrp* was assembled into the vector pBSE402 by using the Golden Gate cloning method. The individual read frame green fluorescent protein (GFP) was used as a reporter gene by the constitutive CaMV 35S promoter in *CmeBrp*-OE and *CmeBrp*-cr vectors. These vectors were transformed into *A. rhizogenes* Ar.Qual (catalog number AC1060).

Peeled melon seeds were sterilized with 75% (v/v) ethanol for 30 seconds, followed by 0.3% (v/v) sodium hypochlorite solution for 15 minutes. The sterilized seeds were germinated on MS30 medium at 28°C for 2 days in darkness before the seedlings were grown at 25°C for 1 week under a 16-h light/8-h dark photoperiod until the cotyledons were fully expanded. Cotyledons were cut off at the basal and tip ends, and soaked in diluted *A. rhizogenes* strain containing the binary vector at 28°C for 20 minutes, then co-cultured on MS solid medium for 2 days in darkness at 23°C. To regenerate roots, explants were transferred to MS solid medium containing 100 mg/l Timentin for 2 weeks at 25°C under a 16-h light/8-h dark photoperiod. Positive roots with GFP fluorescence at ~2 cm length were collected for subsequent experiments. In order to meet the dosage of samples and consistency of biological replications in subsequent experiments, we had to mix four or five roots as a single biological replication.

Ultrapformance liquid chromatography analysis of cucurbitacins B from melon

Ultrapformance liquid chromatography (UPLC) analysis of CuB was performed as described by Zhou *et al.* [18]. Samples were flash-frozen in liquid nitrogen and ground to powder. The resulting powder (0.1 g) was added to methanol (1 ml) and homogenized for 15 min, followed by centrifugation at 10 000 g at 4°C for 10 minutes. The solution was filtered through a 0.22- μ m membrane prior to injection and then analyzed on an HPLC system.

Real-time quantitative PCR

Total RNA was isolated from hairy roots of WT, *CmeBrp*-cr, and *CmeBrp*-OE lines using a Quick RNA Isolation Kit (Huayueyang), and samples of 1 μ g were reverse-transcribed using a GoScript™ Reverse Transcription Mix, Oligo(dT) (Promega, A2791, USA) according to the instruction manual. Then a quantitative PCR assay was performed on an ABI 7900 (Applied Biosystems) machine using GoTaq® qPCR Master Mix Kit (Promega, A6001, USA) according to the manufacturer's instructions. Three independent biological replicates were performed. Relative gene expression was determined using the $2^{-\Delta\Delta CT}$ method and the *ubiquitin* gene (MELO3C009513) was

used as the reference gene [54]. Primers are listed in Supplementary Data Table S8.

Acknowledgements

This work was supported by the National Natural Science Foundation of China (32130093 to Z.Z., 31772304 to Z.Z.) and the National Key R&D Program of China (2016YFD0100307). This work was also supported by the Taishan Scholar Foundation of the People's Government of Shandong Province and the Chinese Academy of Agricultural Science (ASTIP-CAAS and CAAS-XTX2016001), the Shenzhen Municipal (The Peacock Plan KQTD2016113010482651), and the Central Public-interest Scientific Institution Basal Research Fund (No. Y2017PT52).

Author contributions

Y.X. participated in the design of the research, performed the data analysis, and wrote the manuscript. H.Z. designed the experiments. Y.X., Y.Z. and N.J. performed the experiments. X.Z. and Q.Z. collected genome and RNA sequencing data. H.L. and S.C. revised the manuscript. Z.Z. conceived and designed the research, and revised the manuscript. All authors read and approved the manuscript.

Data availability

All data supporting the results of this article are included within the article and its additional files.

Conflict of interests

The authors declare that they have no conflict of interest.

Supplementary data

Supplementary data is available at *Horticulture Research* online.

References

- Riechmann JL, Heard J, Martin G et al. Arabidopsis transcription factors: genome-wide comparative analysis among eukaryotes. *Science*. 2000;**290**:2105.
- Feller A, Machemer K, Braun EL et al. Evolutionary and comparative analysis of MYB and bHLH plant transcription factors. *Plant J*. 2011;**66**:94–116.
- Carretero-Paulet L, Galstyan A, Roig-Villanova I et al. Genome-wide classification and evolutionary analysis of the bHLH family of transcription factors in *Arabidopsis*, poplar, rice, moss, and algae. *Plant Physiol*. 2010;**153**:1398–412.
- Pires N, Dolan L. Origin and diversification of basic-helix-loop-helix proteins in plants. *Mol Biol Evol*. 2010;**27**:862–74.
- Toledo-Ortiz G, Huq E, Quail PH. The *Arabidopsis* basic/helix-loop-helix transcription factor family. *Plant Cell*. 2003;**15**:1749–70.
- Li X, Duan X, Jiang H et al. Genome-wide analysis of basic/helix-loop-helix transcription factor family in rice and *Arabidopsis*. *Plant Physiol*. 2006;**141**:1167–84.
- Wang J, Sun P, Li Y et al. An overlooked Paleotetraploidization in Cucurbitaceae. *Mol Biol Evol*. 2018;**35**:16–26.
- Sun H, Wu S, Zhang G et al. Karyotype stability and unbiased fractionation in the paleo-allotetraploid *Cucurbita* genomes. *Mol Plant*. 2017;**10**:1293–306.
- Dong H, Zhao H, Li S et al. Genome-wide association studies reveal that members of bHLH subfamily 16 share a conserved function in regulating flag leaf angle in rice (*Oryza sativa*). *PLoS Genet*. 2018;**14**:e1007323.
- Yang F, Wang Q, Schmitz G et al. The bHLH protein ROX acts in concert with RAX1 and LAS to modulate axillary meristem formation in *Arabidopsis*. *Plant J*. 2012;**71**:61–70.
- Paik I, Kathare PK, Kim J-I et al. Expanding roles of PIFs in signal integration from multiple processes. *Mol Plant*. 2017;**10**:1035–46.
- Radoeva T, Lokerse AS, Llavata-Peris CI et al. A robust auxin response network controls embryo and suspensor development through a basic helix loop helix transcriptional module. *Plant Cell*. 2019;**31**:52–67.
- Ren Y, Zhao Q, Zhao X et al. Expression analysis of the *MdClbHLH1* gene in apple flower buds and seeds in the process of dormancy. *Hortic Plant J*. 2016;**2**:61–6.
- Zhang HB, Bokowiec MT, Rushton PJ et al. Tobacco transcription factors NtMYC2a and NtMYC2b form nuclear complexes with the NtJAZ1 repressor and regulate multiple jasmonate-inducible steps in nicotine biosynthesis. *Mol Plant*. 2012;**5**:73–84.
- Shen Q, Lu X, Yan T et al. The jasmonate-responsive AaMYC2 transcription factor positively regulates artemisinin biosynthesis in *Artemisia annua*. *New Phytol*. 2016;**210**:1269–81.
- Ribeiro B, Lacchini E, Bicalho KU et al. A seed-specific regulator of triterpene saponin biosynthesis in *Medicago truncatula*. *Plant Cell*. 2020;**32**:2020–42.
- Shang Y, Ma Y, Zhou Y et al. Biosynthesis, regulation, and domestication of bitterness in cucumber. *Science*. 2014;**346**:1084–8.
- Zhou Y, Ma Y, Zeng J et al. Convergence and divergence of bitterness biosynthesis and regulation in Cucurbitaceae. *Nat Plants*. 2016;**2**:16183.
- Xi H, He Y, Chen H. Functional characterization of *SmbHLH13* in anthocyanin biosynthesis and flowering in eggplant. *Hortic Plant J*. 2021;**7**:73–80.
- Massari ME, Murre C. Helix-loop-helix proteins: regulators of transcription in eukaryotic organisms. *Mol Cell Biol*. 2000;**20**:429–40.
- Sun H, Fan HJ, Ling HQ. Genome-wide identification and characterization of the bHLH gene family in tomato. *BMC Genomics*. 2015;**16**:9.
- Heim MA, Jakoby M, Werber M et al. The basic helix-loop-helix transcription factor family in plants: a genome-wide study of protein structure and functional diversity. *Mol Biol Evol*. 2003;**20**:735–47.
- Kane J, Freeling M, Lyons E. The evolution of a high copy gene array in *Arabidopsis*. *J Mol Evol*. 2010;**70**:531–44.
- Fang L, Cheng F, Wu J et al. The impact of genome triplication on tandem gene evolution in *Brassica rapa*. *Front Plant Sci*. 2012;**3**:261.
- Wang N, Cui Y, Liu Y et al. Requirement and functional redundancy of Ib subgroup bHLH proteins for iron deficiency responses and uptake in *Arabidopsis thaliana*. *Mol Plant*. 2013;**6**:503–13.
- Cui Y, Chen C-L, Cui M et al. Four IVa bHLH transcription factors are novel interactors of FIT and mediate JA inhibition of iron uptake in *Arabidopsis*. *Mol Plant*. 2018;**11**:1166–83.

27. Yu J, Ke T, Tehrim S et al. PTGBase: an integrated database to study tandem duplicated genes in plants. *Database (Oxford)*. 2015;**2015**:bav017.
28. Qiao X, Li Q, Yin H et al. Gene duplication and evolution in recurring polyploidization-diploidization cycles in plants. *Genome Biol*. 2019;**20**:38.
29. Frey M, Chomet P, Glawischnig E et al. Analysis of a chemical plant defense mechanism in grasses. *Science*. 1997;**277**: 696–9.
30. Qi X, Bakht S, Leggett M et al. A gene cluster for secondary metabolism in oat: implications for the evolution of metabolic diversity in plants. *Proc Natl Acad Sci USA*. 2004;**101**: 8233–8.
31. Hen-Avivi S, Savin O, Racovita RC et al. A metabolic gene cluster in the wheat W1 and the barley Cer-cqu loci determines β -diketone biosynthesis and glaucousness. *Plant Cell*. 2016;**28**: 1440–60.
32. Winzer T, Gazda V, He Z et al. A *Papaver somniferum* 10-gene cluster for synthesis of the anticancer alkaloid noscapine. *Science*. 2012;**336**:1704–8.
33. Shoji T, Yuan L. ERF gene clusters: working together to regulate metabolism. *Trends Plant Sci*. 2021;**26**:23–32.
34. Nutzmans HW, Huang A, Osbourn A. Plant metabolic clusters – from genetics to genomics. *New Phytol*. 2016;**211**:771–89.
35. Nutzmans HW, Doerr D, Ramírez-Colmenero A et al. Active and repressed biosynthetic gene clusters have spatially distinct chromosome states. *Proc Natl Acad Sci USA*. 2020;**117**: 13800–9.
36. Van Moerkercke A, Steensma P, Schweizer F et al. The bHLH transcription factor *BIS1* controls the iridoid branch of the monoterpenoid indole alkaloid pathway in *Catharanthus roseus*. *Proc Natl Acad Sci USA* 2015;**112**:8130–5.
37. Van Moerkercke A, Steensma P, Gariboldi I et al. The basic helix-loop-helix transcription factor *BIS2* is essential for monoterpenoid indole alkaloid production in the medicinal plant *Catharanthus roseus*. *Plant J*. 2016;**88**:3–12.
38. Singh SK, Patra B, Paul P et al. *BHLH IRIDOID SYNTHESIS 3* is a member of a bHLH gene cluster regulating terpenoid indole alkaloid biosynthesis in *Catharanthus roseus*. *Plant Direct*. 2021;**5**:e00305.
39. Kumar S, Stecher G, Tamura K. MEGA7: molecular evolutionary genetics analysis version 7.0 for bigger datasets. *Mol Biol Evol*. 2016;**33**:1870–4.
40. Kent WJ. BLAT—the BLAST-like alignment tool. *Genome Res*. 2002;**12**:656–64.
41. Hu B, Jin J, Guo AY et al. GSDS 2.0: an upgraded gene feature visualization server. *Bioinformatics*. 2015;**31**:1296–7.
42. Bailey TL, Williams N, Misleh C et al. MEME: discovering and analyzing DNA and protein sequence motifs. *Nucleic Acids Res*. 2006;**34**:W369–73.
43. Wang Y, Tang H, DeBarry J et al. MCScanX: a toolkit for detection and evolutionary analysis of gene synteny and collinearity. *Nucleic Acids Res*. 2012;**40**:e49–e49.
44. Chen C, Chen H, Zhang Y et al. TBtools: an integrative toolkit developed for interactive analyses of big biological data. *Mol Plant*. 2020;**13**:1194–202.
45. Cheng F, Wu J, Fang L et al. Syntenic gene analysis between *Brassica rapa* and other Brassicaceae species. *Front Plant Sci*. 2012;**3**:198.
46. Wang D, Zhang Y, Zhang Z et al. KaKs_Calculator 2.0: a toolkit incorporating gamma-series methods and sliding window strategies. *Genomics Proteomics Bioinformatics*. 2010;**8**: 77–80.
47. Li Z, Zhang Z, Yan P et al. RNA-Seq improves annotation of protein-coding genes in the cucumber genome. *BMC Genomics*. 2011;**12**:540.
48. Yano R, Nonaka S, Ezura H. Melonnet-DB, a grand RNA-Seq gene expression atlas in melon (*Cucumis melo* L.). *Plant Cell Physiol*. 2018;**59**:e4.
49. Guo S, Zhao S, Sun H et al. Resequencing of 414 cultivated and wild watermelon accessions identifies selection for fruit quality traits. *Nat Genet*. 2019;**51**:1616–23.
50. Wu S, Shamimuzzaman M, Sun H et al. The bottle gourd genome provides insights into Cucurbitaceae evolution and facilitates mapping of a *Papaya ring-spot virus* resistance locus. *Plant J*. 2017;**92**:963–75.
51. Jiang B, Xie D, Liu W et al. De novo assembly and characterization of the transcriptome, and development of SSR markers in wax gourd (*Benicasa hispida*). *PLoS One*. 2013;**8**: e71054.
52. Cui J, Yang Y, Luo S et al. Whole-genome sequencing provides insights into the genetic diversity and domestication of bitter melon (*Momordica* spp.). *Hortic. Res.* 2020;**7**: 85.
53. Pertea M, Kim D, Pertea GM et al. Transcript-level expression analysis of RNA-seq experiments with HISAT. *StringTie and Ballgown*. *Nat Protoc*. 2016;**11**:1650–67.
54. Wang S, Yang X, Xu M et al. A rare SNP identified a TCP transcription factor essential for tendril development in cucumber. *Mol Plant*. 2015;**8**:1795–808.